Low-cost Setup for Electromagnetic SAR Evaluation in a Human Phantom

S.I. Rodríguez*, A. Gallego*, E. Pineda*, J.C. Vargas†,M.R. Pérez‡, F. Román*, and J.L. Araque*
* Universidad Nacional de Colombia, Ciudad Universitaria, Bogotá 111321, Colombia
†Hospital Universitario Nacional de Colombia
‡Dept. of Electronics Engineering, Pontificia Universidad Javeriana, Bogotá, Colombia
Corresponding author: jlaraqueq@unal.edu.co

***Abstract*—We describe a low-cost setup developed to carry out SAR measurements on a human phantom. The development comprises: a human phantom manufactured using a modified workflow from the mannequin industry, liquid preparations using recipes found in the literature, a system for the transmission and reception of RF signals, a system for tracking the position of a field probe during the scanning, which is carried out manually, and a system for the integration and post-processing of the measured data. Preliminary validation results demonstrate good performance for all the blocks described. Detailed results from an underway measurement campaign with these blocks will be presented during the conference.**

***Index Terms*—Tissue modeling fluid, experimental phantom, specific absorption rate (SAR), software defined radio, position tracking.**

I. INTRODUCTION

In the light of a wide deployment of 5G infrastructure and a widespread adoption of the associated mobile terminals, regulatory agencies are striving to insure that compliance testing is accurate [1]. The International Telecommunication Union (ITU) and the World Health Organization (WHO), among others have issued documents providing guidance and dissemination on the subject and existing standards. Nevertheless, the community's perception of risk is escalating, mainly due to misinformation, including among others, unsubstantiated claims that 5G systems are much riskier than their predecessors. In this context, the project "EM Fields by 5G Systems and Human Health, Study in the Colombian Context", funded by the Agencia Nacional del Espectro, brings together technical and scientific knowledge and a multidisciplinary work contextualized to the National case for a multi-perspective analysis of the forthcoming deployments of the 5G technology in Colombia, and aims at generating recommendations for an appropriate balance between the user experience of new services, people's health, and the community's perception of risk. The present contribution describes the experimental setup developed for the evaluation of the Electromagnetic Specific Absorption Rate (SAR) in a human model (phantom), which is one of the work packages of the project.

This paper is organized as follows. In Section II, a SAR measurement background is presented. In Section III, detailed architecture of the system is described. A preliminary validation results, and some final conclusions and future work are presented in Sections IV and V, respectively.

This work is funded by the Agencia Nacional de Espectro, Colombia (ANE), convocatoria de investigaciones 2021, contract 115-2021

II. BACKGROUND

A. SAR measurement

The Specific Absorption Rate (SAR) is defined as the measure of the rate of absorption of Radio Frequency (RF) electromagnetic energy by the human body. [2], and can be determined according to these formulas:

$$SAR = \frac{\sigma E^2}{\rho} \quad (1)$$

$$SAR = C_h \left.\frac{\partial T}{\partial t}\right|_{t=0} \quad (2)$$

where:

- SAR is the Specific Absortion Rate in W/kg
- E is the RMS value of the electric field intensity in V/m
- σ is the electrical conductivity of the tissue in S/m
- P is the mass density of the tissue in $\mathrm{kg/m^3}$
- C_h is the specific heat capacity of the tissue in $\mathrm{J/kg/^\circ K}$
- t is time in s
- T is the temperature in $^\circ K$

The minimum SAR evaluation setup requires a representation of the EM properties and shape of the human body (human tissue-emulating material and its container, called phantom), an isotropic E-field probe, and an RF transmitter and receiver. When a 3D representation of the SAR in several positions inside a phantom is required, the probe moves inside a liquid, and the E-field measurement probe must be associated at all times with a 3D position vector, and an additional rotation information when the individual field components are of interest.

Current isotropic E-field probes that required for this near-field measurements have several limitations in terms of operation frequency and spatial resolution [3]. This limitation only increases when commercial options for SAR probes require additional equipment whose cost is above tens of thousands of dollars. The same scenario applies for tissue simulating liquids, phantoms, software and positioning systems, which are usually robotic arms. The most advanced commercial platform is offered by SPEAG, Exposure Adquisition System (EASY6), probes, broad-band tissue simulating liquids and complete measurement equipment and software (DASY8), which includes a robotic arm positioning system. Similar assesment systems like ALSAS-10U also provide a complete test solution including even certified phantoms [4], [5]. Regarding the positioning system, robot arms are the only commercial solution available and have been recommended for long time [6]. While these afford an effortless and accurate measurement workflow, the system has very high cost, and poses the risk of damaging the probe or the inability to configure sweeps on the phantom of other measurement medium when it is not correctly accounted for within the control software, often difficult to customize. However, in [7] a methodology for a hanheld probe antenna in E-field pattern diagnostics was described. The tracking system used several infrared cameras and reflectors in order to pinpoint the location of the probe with a resolution under 0.1 mm, offered commercially. Similar approaches have been taken in other contexts where free-standing equipment must be tracked [8]. The general idea allows fast execution of field measurements and is a valuable replacement for robotic arms given the context-accurate an adaptive operation inherent to human operators, which adds up to the considerable cost savings.

With 5G systems and the utilization of millimeter-wave (mm-Wave) bands, along with beam-steerable phased array antennas, the complexity of the testing scenarios has increased, and the SAR measurement techniques are extremely time-consuming and require considerable budget. As an alternative, we have undertaken the development of a cost-effective standards-compliant SAR testing system, employing E-field probes and a human operator for the spatial sweep, which is tracked by an optical system developed in-house.

III. Description and Initial Validation of the System

The general block description of the system is in fig. 1. it starts with the signal generation and adquisition systems USRP B210, the Horn antenna, the probe support and probe tip, the two low cost cameras and three MATLAB instances running transmitting channel, receiving channel and the tracking system software. Once the probe tip is attached to the LED-based support and this is being moved by a person, the near-field of the antenna is measured and the 3D position is adquired simultaneously. Although this information has still to be processed offline, they both contain a time vector up to milliseconds acccuracy and were configured both at 20 samples per second.

A. Human phantom and filling material

To make a model that simulates human tissue, it is necessary to develop both the container and the preparation that will simulate its electrical properties. For the preparation that will simulate human tissue, we are based on the IEC/IEEE 62209-1528-2020 standard. There, the electrical parameters that must be met for the preparation are specified. Among these parameters is the electrical permittivity of the preparation as well as the conductivity. These values can be seen in the Table I. For the scope of our project, focused on the 5G frequencies to be used in Colombia, we consider the material permittivity and conductivity at 3.5 GHz, which appear in the Table I highlighted in blue.

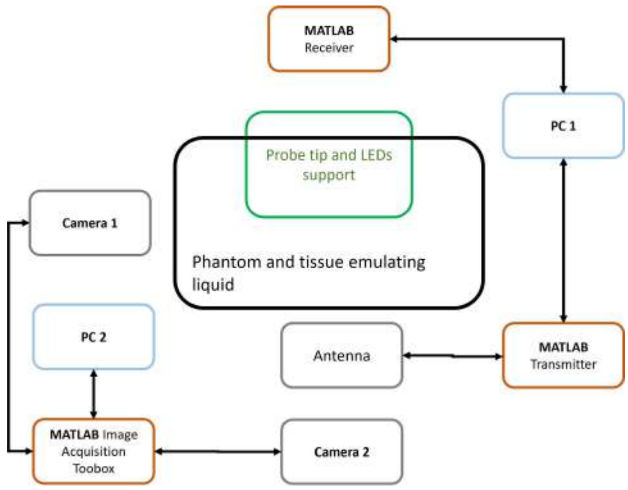

Fig. 1. Block diagram of the setup for Electromagnetic SAR evaluation in a phantom.

Fig. 2. Setup for measurement of dielectric properties

To achieve this, the preparation carried out by Benjamin Loader was used as a guide [9], whereby using water, polysorbate 20 and salt, in different proportions, the electrical conditions of the human head tissue are recreated. The preparation was measured using an electrical permittivity measurement equipment which consists of a DAK 3.5 probe, an Anritsu Master MS2028C spectrum analyzer and a computer, as can be seen in the Fig. 2; these measurements where carried out at the Electronics Engineering Laboratory at the Pontificia Universidad Javeriana. This equipment has its own calibration kit (Short - Open - Load), where the Load is a liquid developed by the manufacturer of the DAK 3.5 open coaxial probe (SPEAG).

The human phantom was manufactured by a modified workflow used in the mannequin industry, which is shown

Fig. 3. Container developed for the project (Mannequin)

TABLE I
ELECTRICAL CHARACTERISTICS OF THE FABRIC BETWEEN 4 MHZ AND 10 GHZ. IEC/IEEE 62209-1528-2020 STANDARD AT $20°C$

Frequency MHz	*Real part of the complex relative permittivity,*	*Conductivity,*	*Penetration depth (E-field),*
4	55,0	0,75	293,0
13	55,0	0,75	165,5
30	55,0	0,75	112,8
150	52,3	0,76	62,0
300	45,3	0,87	46,1
450	43,5	0,87	43,0
750	41,9	0,89	39,8
835	41,5	0,90	39,0
900	41,5	0.97	36,2
1450	40,4	1.20	28,6
1800	40.0	1,40	24,3
1900	40,0	1,40	24,3
1950	40,0	1,40	24,3
2000	40,0	1,40	24,3
2100	39,8	1,49	22,8
2450	39,2	1,80	18,7
2600	39,0	1,96	17,2
3000	38,5	2,40	14,0
3500	**37,9**	**2,91**	**11,4**
4000	37,4	3,43	10,0
4500	36,8	3,94	9,7

in Fig. 3. This phantom displays a detailed human silhouette and is thin enough (3mm) to enable accurate measurements of SAR.

The material from which the mannequin is made (fiberglass), was characterized in order to assess its impact on the SAR measurement; using a specially prepared sample, and the equipment mentioned above, we confirmed a low dielectric constant and loss tangent in the band of interest.

Table I shows the electrical permittivity value of the IEC/IEEE 62209-1528-2020 standard. The value at 3.5 GHz is highlighted in blue, which is the reference against which our results will be compared.

The data collected in the measurement are shown in Fig. 4 and 5. We note that these measurements show a very good correspondence with the standard at the frequency of interest, denoted by an X marker. The materials tested were:

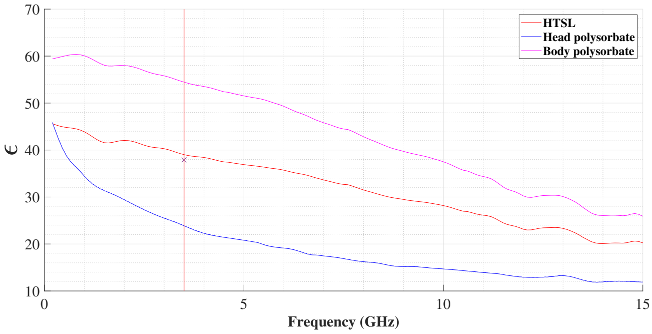

Fig. 4. Electric permittivity measurement. Epsilon HTSL (Head Tissue Simulating Liquids), head polysorbate and body polysorbate. Real part

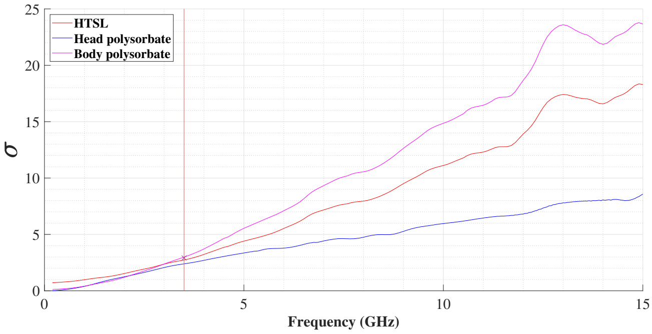

Fig. 5. Conductivity measurement. Sigma HTSL (Head Tissue Simulating Liquids), head polysorbate and body polysorbate. Real part

the standard fluid provided by SPEAG for its SAR acquisition system, and two preparations we made to model different body tissues (head and generic body).

B. Equipment and control

1) Signal generation and acquisition: Two Universal Software Radio Peripheral (USRP) B210 connected to a PC through the USB3 interface have been used, one on the side of the transmitter and the other on the receiver. The USRP support from Communications Toolbox in MATLAB has been employed for generating a baseband signal that consists of a single tone, and for saving received I/Q samples to a file for further processing. The SDR hardware is configured at 3.5 GHz with a 2 MHz instantaneous data bandwidth. All the baseband processing and algorithmic post-processing are performed in MATLAB. It is worth mentioning that transmitter and receiver run on separate MATLAB instances to prevent bottleneck issues during transceiver mode operation.

2) Position tracking: The tracking system proposed here uses two low-cost webcams, the MATLAB image acquisition toolbox and a probe support with three regular Light Emitting Diodes (LEDs). The idea is to track the position of the red, green and blue lights in 3D alongside a timestamp in a single vector, which then will be sent to the integration platform for the post-processing that allows 3D SAR reconstruction. The use of three collinear LEDs was deemed appropriate for our

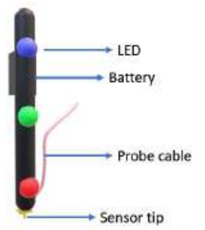

Fig. 6. LED-based probe support for tracking system and coaxial probe model

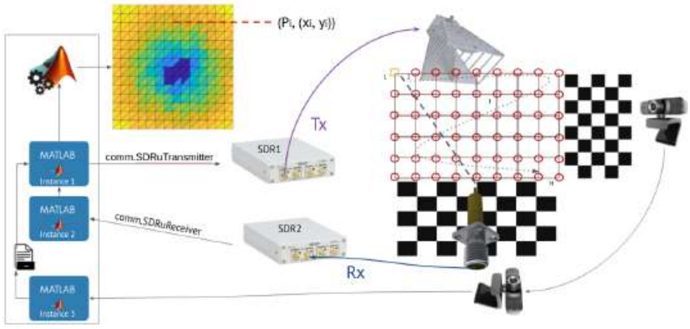

Fig. 7. Test setup and illustration of the overall workflow and data integration.

tests in view of the redundancy these provide, and that the field sensor used is invariant to on-axis rotations.

3) Integration platform: During data acquisition, the system receives I/Q samples from the B210 device and then calculates the peak power and saves a an average value; the power data acquisition subsystem captures 20 samples per second, which is deemed appropriate for a handheld measurement system. The position tracking subsystem operates concurrently at 20 samples per second as well, saving the 3-D position in a file with a timestamp. Later, the post-processing evaluates the raw data, synchronizes the power and position samples, and interpolates all of them in a single dataset. Finally, a two-dimensional graphical output is produced with Delaunay triangulation, which is used before other similar methods because it tends to avoid extremely acute angles for the triangles forming the desired 2D mesh, and is considered a fast triangulation algorithm also. in relative power dB values. The SDR architecture affords a simple configuration of the experiment, from single-tone excitation to elaborated MIMO broadband tests as those of interest in 5G systems.

IV. System Test

A simple scanning of the near field at the aperture of the LB-880-NF ridged horn antenna with aperture size 28.4cm x 18.6cm was performed. The test was carried out within a shielded chamber in the EMC Lab at Universidad Nacional de Colombia. The 1-D E-field probe consist on a coax probe linearly polarized monopole connected to the receiving port, which is swept manually. Even though the system is able to perform 3-D measurements, in this case, the scanning has been performed in the 2-D plane surface facing the horn aperture as in fig. 7.

During the test, the probe located within the support (see Fig. 6) is held in a configuration co-polarized with the antenna under test (AUT) and moved alongside a plane close to its aperture. The two webcams are connected to a laptop to capture the position of the LEDs, extrapolate the position of the probe tip and timestamp the information for further processing. The equipment and some aspects of the setup are shown in Fig. 8.

About 400 position points are calculated in Fig. 9 and were acquired in a time interval of 20 seconds and saved in a vector with data accuracy in the order of mm and ms from our initial tests.

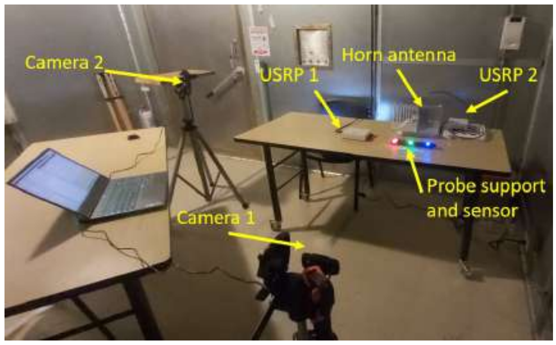

Fig. 8. Experimental setup for RF power distribution of a horn antenna with a hand held positioning system.

Fig. 10 presents the relative (uncalibrated) power map in X-Y coordinates; the dashed line represent the boundary of the antenna. It can be observed that the RF power is higher at the center of the antenna, as expected for the dominant mode, and decays close towards the left and right edges. Some asymmetries are visible, due to aspects of the setup that we are currently improving, including the probe support and the surroundings of the horn aperture.

Finally, table II shows a comparison between the proposed

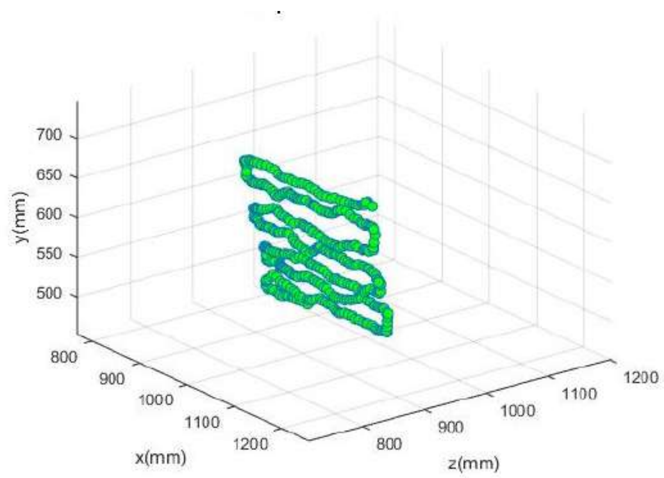

Fig. 9. Probe 3D positions in front of the horn antenna.

TABLE II
RESOLUTION, COST AND ACCURACY COMPARISON OF THE PROPOSED SYSTEM AND SPEAG'S DASY8 COMMERCIAL SAR MEASUREMENT SETUP.

Setup		Samples/ s	Spatial resolution and measurement range	Software	Cost (USD) (Approx.)
Proposed system	In-home probe tracking and positioning	20	2mm in a 2m x 2m x 1m volume	Matlab	50
	2 USRP B210	20	N/A	Matlab	3.870
	EASY6-EX3DV4	>20	<1 mm and 5uW/g	Speag	21.000
	2 PCs	>20	N/A	Matlab	1.500
	Phantom				400
	Tissue emulating liquid				400
					27.220
DASY8-EX3DV4 with robot arm		16	<1 mm with a 920 mm reach and 5uW/g	Speag	400.000

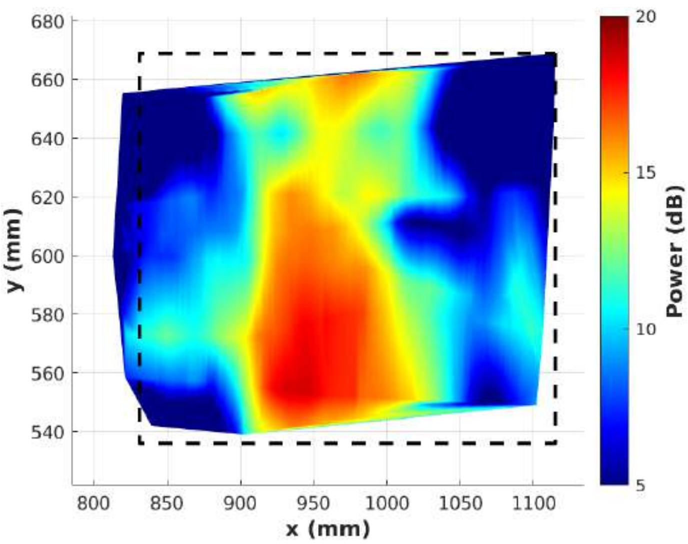

Fig. 10. RF power distribution heat map of the double-ridged horn aperture test (physical aperture area defined by the dashed line).

system and DASY8. With the same spatial resolution and measurement range values (both experiments include the EASY6 probe), and as there is no need for a robot arm with a handheld positioning and tracking system, our system costs 14 times less than accepted systems. Additionally, the proposed LED-based probe support could handle more samples per second and positioning area.

V. CONCLUSIONS AND FUTURE WORK

The preliminary validation results show the feasibility of a low cost setup for the measurement of SAR. The material properties of the phantom and the filling materials were found appropriate at the band of interest and on a broader band, too. The equipment control and units show satisfactory accuracy in the positioning and timing with 2 mm spatial resolution and 20 samples per second. Current work is focused on the integration of a standards-compliant isotropic E-field probe and a measurement campaign of the complete system, including a 3-D sweep inside the anatomical model developed, and will be reported during the Conference.

ACKNOWLEDGMENT

This work was funded by the Agencia Nacional del Espectro, Colombia, in the framework of Convocatoria de investigaciones 2021, contract 115-2021.

REFERENCES

[1] B. Beard, W. Kainz, T. Onishi, T. Iyama, S. Watanabe, O. Fujiwara, J. Wang, G. Bit-Babik, A. Faraone, J. Wiart, A. Christ, N. Kuster, A.-K. Lee, H. Kroeze, M. Siegbahn, J. Keshvari, H. Abrishamkar, W. Simon, D. Manteuffel, and N. Nikoloski, "Comparisons of computed mobile phone induced SAR in the SAM phantom to that in anatomically correct models of the human head," *IEEE Transactions on Electromagnetic Compatibility*, vol. 48, no. 2, pp. 397–407, 2006.

[2] IEC and I. I. Standard, "Iec/ieee 62209-1528, measurement procedure for the assessment of specific absorption rate of human exposure to radio frequency fields from hand-held and body-worn wireless communication devices—human models, instrumentation and procedures (frequency range of 4 mhz to 10 ghz)," 2020.

[3] K. Pokovic, T. Schmid, and N. Kuster, "Millimeter-resolution E-field probe for isotropic measurement in lossy media between 100 MHz and 20 GHz," *IEEE Transactions on Instrumentation and Measurement*, vol. 49, no. 4, pp. 873–878, 2000.

[4] Speag, "Dasy8 systems," 2021. [Online]. Available: https://speag.swiss/products/dasy8/overview/

[5] DASY8, "Dasy8 module sar/apd," 2021. [Online]. Available: https://speag.swiss/products/dasy8/m-sar-apd/

[6] T. Schmid, O. Egger, and N. Kuster, "Automated E-field scanning system for dosimetric assessments," *IEEE Transactions on Microwave Theory and Techniques*, vol. 44, no. 1, pp. 105–113, 1996.

[7] G. Álvarez Narciandi, J. Laviada, Y. Álvarez López, G. Ducournau, C. Luxey, C. Belem-Goncalves, F. Gianesello, N. Nachabe, C. D. Rio, and F. Las-Heras, "Freehand system for antenna diagnosis based on amplitude-only data," *IEEE Transactions on Antennas and Propagation*, vol. 69, no. 8, pp. 4988–4998, 2021.

[8] G. Virone, A. M. Lingua, M. Piras, A. Cina, F. Perini, J. Monari, F. Paonessa, O. A. Peverini, G. Addamo, and R. Tascone, "Antenna pattern verification system based on a micro unmanned aerial vehicle (uav)," *IEEE Antennas and Wireless Propagation Letters*, vol. 13, pp. 169–172, 2014.

[9] B. G. Loader, A. P. Gregory, and R. Mouthaan, "Formulation and properties of liquid phantoms, 1 mhz to 10ghz," NPL Report, May 2018. [Online]. Available: http://eprintspublications.npl.co.uk/7946/